Topographic and vegetation effects on snow accumulation in the southern Sierra Nevada: a statistical summary from Lidar data

Z. Zheng[1], P. B. Kirchner[2,3], R. C. Bales[1,4]

[1] Department of Civil and Environmental Engineering, UC Berkeley, Berkeley, CA, USA

[2] Joint Institute for Regional Earth System Science and Engineering, Pasadena, CA, USA

[3] Southwest Alaska Network, National Park Service, Anchorage, AK, USA

[4] Sierra Nevada Research Institute, UC Merced, Merced, CA, USA

Correspondence to: Z. Zheng (zeshi.z@berkeley.edu)

Abstract

Airborne light detection and ranging (Lidar) snow-on and snow-off measurements collected in the southern Sierra Nevada near peak snow accumulation and in the snow-free season in the 2010 water year were analyzed for topographic and vegetation effects on snow accumulation. Combining point-cloud data from four sites separated by 10 to 64 km, with total surveyed area over 106 km^2, it was observed in that the mixed-conifer forest the percent of pixels with snow-depth measurments is sensitive to the sampling resolution used in processing the point cloud. This is apparently due to Lidar not receiving returns from under the denser canopy. From the 1-m gridded data, it was observed that in addition to elevation effects, snow depth has a strong dependency on slope, aspect and canopy penetration fraction. A multivariate linear model built using all physiographic variables explained 15 to 25% more variability in snow depth than did a univariate linear model with elevation as a single predictor. However, the weight that each physiographic variable exerted on snow depth varied across different elevation ranges, as well as with different canopy-cover amounts. The difference between mean snow depth measured in open area and under canopy increased with elevation in rain-snow transition zone from 1500 to 1800 m and stabilized at about 25 to 45 cm above about 2000 m elevation, with the range reflecting the effects of other topographic variables.

1. Introduction

In the western United States, ecosystem processes and water supplies for agricultural and domestic use depend on the mountain snowpack as the primary source of late-spring and early summer streamflow (Bales et al., 2006). Knowledge of spring snowpack conditions within a watershed is essential if water availability and flood peaks following the onset of melt are to be accurately predicted (Hopkinson et al., 2001). Both topographic and vegetation factors are important in influencing the snowpack conditions, as they closely interact with meteorological conditions to affect precipitation and snow accumulation distribution in the mountains (McMillen, 1988; Raupach, 1991; Wigmosta et al., 1994). However, the distribution of mountain precipitation is poorly understood at multiple spatial scales because it is governed by processes that are neither well measured nor accurately predicted (Kirchner et al., 2014). Snow accumulation across the mountains is primarily influenced by orographic processes, involving feedbacks between atmospheric circulation and terrain (Roe, 2005; Roe and Baker, 2006). In most forested regions, snow accumulation is highly sensitive to vegetation structure (Anderson, 1963; Revuelto et al., 2015; Musselman et al., 2008), and canopy interception, sublimation and unloading result in less accumulation of snow beneath the forest canopies in comparison with canopy gaps (Mahat and Tarboton, 2013).

The Sierra Nevada is ideally suited for studying mountain snow distribution and related hydrologic processes because it serves as a barrier to moisture moving inland from the Pacific, has an ideal orientation for producing orographic precipitation, and thus exerts a strong influence on the upslope amplification of precipitation (Colle, 2004; Rotach and Zardi, 2007; Smith and Barstad, 2004). Recent studies have revealed some insights of snow-depth dependency on orographic and topographic effects in the Alps (Grünewald et al., 2013; Grünewald, et al., 2014;

52 Lehning et al., 2011), suggesting that similar studies could be extended to the Sierra Nevada.
53 And among the forested regions of the mountains, the mixed-conifer and subalpine zones cover
54 most of the high-elevation, seasonally snow-covered area.

55 Manual snow surveys, one-time surveys, and remote-sensing products are used to
56 estimate precipitation and snow accumulation in the Sierra Nevada (Guan et al., 2013). *In situ*,
57 operational measurements of snow water equivalent (SWE) come from monthly manual snow
58 surveys and daily snow pillow observations (Rosenberg et al., 2011). Cost, data coverage,
59 accuracy (Julander et al., 1998) and basin-scale representativeness are issues for *in situ*
60 monitoring of SWE in mountainous terrain (Rice and Bales, 2010). Satellite-based remote
61 sensing, such as MODIS, has been used to map snow coverage in large or even global areas.
62 However, it only provides snow-coverage information in canopy gaps, and no direct information
63 on snow depths (Molotch and Margulis, 2008). There is also the SNOw Data Assimilation
64 Systems (SNODAS) that integrate data from satellite and *in situ* measurements into a physical
65 snowpack model, which provides SWE and snow-depth estimates (Barrett, 2003). However,
66 since SNODAS has not been broadly evaluated (Clow et al., 2012), its potential for studying the
67 snow distribution in mountainous areas remains uncertain. Also, owing to its 1-km spatial
68 resolution, the snow depth that SNODAS provides is a mixed representation of both open and
69 canopy-covered areas. An orographic-lift effect is observable in most of the above data (Howat
70 and Tulaczyk, 2005; Rice et al., 2011), and a binary-regression-tree model using topographic
71 variables as predictors has also been used for estimating the snow depth in unmeasured areas
72 (Erickson et al., 2005; Erxleben et al., 2002; Molotch et al., 2005). However, regression
73 coefficients could not be estimated accurately for most of the predictors, except for elevation,
74 and the consistency of the orographic trend as well as the relative importance of these predictors

is still unknown owing to lacking representative measurements across different slopes, aspects and canopy conditions. And the stability of the variance explained by the model also needs to be tested with denser measurements.

In recent years, airborne Lidar has been employed for high-spatial-resolution distance measurements (Hopkinson et al., 2004), and has become an important technique to acquire topographic data with sub-meter resolution and accuracy (Marks and Bates, 2000). Therefore, Lidar provides a potential tool to help understanding spatially distributed snow depth across mountainous regions. With multiple returns from a single laser pulse, Lidar has also been used to construct vegetation structures as well as observe conditions under the canopy, which helps produce fine-resolution digital elevation models (DEMs), vegetation structures, and snow-depth information. However, the snow depth under canopy can not always be measured because of the signal-intensity attenuation caused by canopy interception (Deems and Painter, 2006; Deems et al., 2006). A recent report applied a univariate-regression model to the snow depth measured in open areas using Lidar; with a high-resolution DEM used to accurately quantify the orographic-lift effect on the snow accumulation just prior to melt (Kirchner et al., 2014). From this analysis it could be expected that Lidar data might also help explain additional sources of snowpack distribution variability in complex, forested terrain.

The objective of this work reported here is to improve our understanding of the topographic and vegetation effects on snow accumulation in the mixed-conifer forest. We investigated these by using Lidar data collected in four headwater areas in the southern Sierra Nevada and address the following three questions. First, is it possible to have snow-depth measurements in forested mountain terrain from all pixels on a fine sampling resolution (1 to 5m) using Lidar data? If not, how does the percentage of pixels measured change with the sampling

resolution. Second, what is the importance of slope, aspect and canopy penetration fraction on snow accumulation, relative to elevation; and are effects consistent across sites? Third, what is the snow-depth difference between open and canopy-covered areas; how does it change with elevation; and is the difference stable with respect to other topographic variables?

2. Methods

2.1 Study Areas

Our study areas are located in the southern Sierra Nevada, approximately 80 km east of Fresno, California (Figure 1). The four headwater-catchment research areas, Bull Creek, Shorthair Creek, Providence Creek, and Wolverton Basin were previously instrumented, including meteorological measurements, in order to have a better knowledge of the hydrologic processes in this region (Bales et al., 2011; Hunsaker et al., 2012; Kirchner et al., 2014). The sites were chosen as part of multi-disciplinary investigations at the Southern Sierra Critical Zone Observatory, and are also the main instrumented sites in the observatory. Wolverton is approximately 64 km southeast of the other three sites (Figure 1) and is located in Sequoia National Park. Both snow-on and snow-off airborne Lidar were flown in 2010 (Table 1) over these sites. The elevation of the survey areas is from 1600-m to 3500-m elevation. Vegetation density generally decreases in high-elevation subalpine forest, with Wolverton also having a large area above treeline (Goulden et al., 2012). The precipitation has historically been mostly snow in the cold and wet winters for elevations above 2000 m, and a rain-snow mix below 2000 m, where most of Providence is located. The comparison between Providence and the other sites can help in accessing if observed trends are consistent above and below the rain-snow transition. Also, various elevation spans of sampling sites is important in understanding the stability of the relative importance of physiographic variables across heterogeneous topography.

2.2 Data Collection

All airborne LiDAR surveys were performed by using Optech GEMINI Airborne Laser Terrain Mapper. The scan angle and scan frequency were adjusted to ensure a uniform along-track and across-track point spacing (Table 2), and six GPS ground stations were used for determining aircraft trajectory. The snow-on survey date was close to April 1st, which is used by operational agencies as the date of peak snow accumulation for the Sierra. Since the snow-on survey required four days to cover the four study areas, time-series *in situ* snow-depth data measured continuously from Judd Communications ultrasonic depth sensors at Providence, Bull and Wolverton were used to estimate changes in snow depth during the survey period. While no snow accumulation was observed, snowpack densification and melting observed from the time-series data were taken into considerations (Hunsaker et al., 2012; Kirchner et al., 2014). The snow-off survey was performed in August after snow had completely melted out in the study areas.

2.3 Data Processing

Raw Lidar datasets were pre-processed by NCALM and are available from the NSF Open-Topography website (http://opentopography.org) in LAS format. The LAS point cloud, including both canopy and ground-surface points, are stored and classified as ground return and vegetation return. Each point is also attributed with the total number of returns and position of all returns from its source laser pulse. The 1-m resolution digital-elevation models, generated from the Lidar point-cloud datasets, were downloaded from the OpenTopography database and further processed in ArcMap 10.2 to generate 1-m resolution slope, aspect, and northness raster products. Northness is an index for the potential amount of solar radiation reaching a slope on a scale of -1 to 1, calculated from:

144

145 $$N = \sin(S) \times \cos(A), \quad (1)$$

146

147 where N is the northness value; S is the slope angle of the terrain; and A is the aspect angle.
148 Northness is also the same as the aspect intensity (Kirchner et al., 2014) with 0° focal aspect.
149 Since in this analysis the snow-depth comparison is only discussed between north and south
150 facing slopes, northness is used instead of aspect intensity for simplification. To construct the
151 vegetation structure from Lidar data, points that are from the first return of the laser pulse are
152 used to generate 1-m gridded digital-surface models. And 1-m resolution canopy-height models
153 were built by subtracting the digital-elevation models from the digital-surface models.

154 The snow depths were calculated directly from the snow-on Lidar data. By referring to
155 canopy-height models, all ground points in snow-on Lidar datasets were classified as under
156 canopy or in canopy gaps. That is, if the point was coincident with canopy of >2-m height, it was
157 classified as under canopy, and otherwise in a canopy gap. After classification, snow depths were
158 calculated by subtracting the values in the digital-elevation model from the snow-on point-
159 measurement values. The calculated point snow-depth data were further assigned into 1-m raster
160 pixels, averaged within each pixel, formatted and then gap filled by interpolation with pixel
161 values around it. Since the measurements collected under canopy were insufficient within each
162 pixel (Figure 2) and varied across the transition from the tree trunk to the edge of the canopy,
163 interpolation was not applied to data under the canopy. The error rate of the calculated snow
164 depth should be mainly from the instrumental elevation error, which is about 0.10 m (Kirchner et
165 al., 2014; Nolan et al., 2015).

166 ## 2.4 Penetration Fraction

The open-canopy fraction is a factor that represents the forest density above a given pixel and is used to describe the influence of vegetation on snow accumulation and melt. However there is no algorithm to directly extract this information from Lidar data. Here we use a novel approach we call penetration fraction to approximate the open-canopy fraction from the Lidar point cloud. Penetration fraction is the ratio of the number of ground points to number of total points within each pixel. Because the electromagnetic radiation from both Lidar and sunlight beams are intercepted by canopies, the open-canopy fraction is used here as an index to represent the fraction of sunlight radiance received on the ground under vegetation. Therefore, penetration fraction of Lidar is actually another form of estimating the open-canopy fraction (Musselman et al., 2013). Penetration fraction was calculated as the number of ground points divided by total points in each pixel (Figure 3a). However, under-canopy vegetation can also intercept the Lidar beam causing a bias. To eliminate this bias, the canopy-height model was used to check if the pixel was canopy covered by using a threshold value of 2 m; and if not, the local penetration fraction of the pixel was reset to 1 because the open-canopy fraction of a pixel could not be entirely represented by the penetration fraction. A spatial moving-average process was applied using a 2-D Gaussian filter with a radius of 5 m to account for the effect of the vegetation around each pixel. Finally, we tested the sensitivity of smoothing results to the radius of the filter and found it is not sensitive when the radius is greater than 1.5 m (Figure 3b).

2.5 Statistical Analysis

The 1-m resolution snow-depth raster datasets were resampled into 2-m, 3-m, 4-m and 5-m resolution. The percentage of pixels with snow-depth measurements was calculated by using the number of pixels with valid data divided by the total number of pixels inside each survey area. The sensitivity of the percentage changes across different resampling resolutions and the

consistency of the percentages across study sites at the same resampling resolution were analyzed by visualizing the percentages against sampling resolutions at all sites.

Using elevation, slope, aspect, penetration fraction and snow depth retrieved from Lidar measurements, topographic and vegetation effects on snow accumulation were observed using residual analysis. Owing to orographic effects, there is increasing precipitation along an increasing elevation gradient in this area (Kirchner et al., 2014). Therefore, elevation was selected as the primary variable to fit the linear regression model for calculating the residual of snow depth. All snow-depth measurements from Lidar were first separated by either under canopy or in canopy gaps, and then were binned by elevation of the location where they were measured, with a bin size of 1-m elevation. As each elevation band had hundreds of snow-depth measurements after binning, the average of all snow depths was chosen as the representative snow depth, and the standard deviation calculated to represent the snow-depth variability within each elevation band. Coefficients of determination between snow depth and elevation of each site were calculated by linear regression. The fitted linear regression model of each site was applied to the DEM to estimate the snow depth. The residual of snow depth was calculated by subtracting the modeled snow depth from Lidar-measured snow depth. The slope, aspect and penetration fraction were binned into 1° slope, 1° aspect, and 1% penetration-fraction bins. In this study we treat penetration fraction as a physiographic variable and snow-depth residuals corresponding to each bin of each physiographic variable were averaged and visualized along the variable gradient to check the existence of these physiographic effects.

For the variables found to correlate with the snow accumulation, the relative importance of each variable was calculated using the Random Forest algorithm (Breiman, 2001; Pedregosa and Varoquaux, 2011). A multivariate linear regression model was also fitted into all

physiographic variables to calculate the regression coefficients, which could be used as the quantification of the effect on snowpack distribution from the variable.

To calculate the snow-depth difference between open and canopy-covered area along an elevation gradient, the 1-m resolution snow-depth data of the two conditions, open and canopy-covered, were smoothed separately against elevation using locally weighted scatterplot smoothing (LOESS) (Cleveland, 1979). The snow-depth difference was then calculated by subtracting the smoothed canopy-covered snow depth from that in open.

3. Results

The percentage of pixels that have snow-depth data measured is highly sensitive to the sampling resolution used in processing the Lidar point cloud, which is about 65 to 90% with 1-m resolution and gradually increases to 100% at 5-m resolution (Figure 4). Note that the percentage increases in going from the lower to higher elevation sites, consistent with local forest density decreasing with elevation.

The snow depth in canopy gaps shows a consistent linear trend with elevation across all sites (Figure 5a). The variability (Figure 5b) is highest at about 1500 m, and gradually decreases within rain-snow transition until elevation reaches 2000 m. However, at above 2000 m, the trends of variability changing along elevation gradient vary across sites. In general, snow depth is linearly correlated with elevation at all sites, both in the open area and under the canopy. Note that values at the upper or lower ends of elevation at each site have few pixels and maybe less representative of the value of physiographic attributes in the study areas (Figure 5c). The forested area, of all four sites combined, spans the rain-snow transition zone in mixed conifer through subalpine forest to significant areas above treeline.

For each individual site, a least-squares linear regression of snow depth versus elevation was used to investigate the spatial variability of snow depth. The median elevation of the three sites increases from Providence to Bull to Shorthair. The lowest elevation at Providence Creek is less than 1400 m, and snow depth increases steeply in this region at a rate of 38 cm per 100 m in open areas and 28 cm per 100 m under the canopy. Bull Creek has an elevation range of 2000-2400 meters, which is slightly higher than Providence, and has snow depth increasing at 21 cm per 100 m in open areas and 19 cm per 100 m under the canopy. For Shorthair Creek site, which is the highest of the three, the snow depth increases at 17 cm per 100 m in open areas and 16 cm per 100 m under the canopy. Wolverton is 64 km further south and spans a wide elevation range, going from the rain-snow transition in mixed conifer, to subalpine forest, to some area above treeline. The average snow-depth increase is smallest among all four study sites, 15 cm per 100 m in canopy gaps and 13 cm per 100 m under the canopy. Unlike the other three lower-elevation sites, the snow depth at Wolverton site decreases above 3300-m elevation. The amount of area above this elevation is relatively small, and factors such as wind redistribution and the exhaustion of perceptible water can also affect snow depth at these elevations (Kirchner et al., 2014).

The residuals for the snow in the open areas were further analyzed for effects of slope, aspect and penetration fraction. The snow-depth residual decreases about 10 to 40 cm as slope angle increases from 0° to 60°; and the residual decreases around 50 to 100 cm in going from north-facing to south-facing slopes (Figure 6a, 6b). More interestingly, the topographic effect can be seen from the color pattern of northness observed in the scatterplots (Figure 7a, 7b). The residual increases about 40 to 60 cm as penetration fraction increases from 0% to 80% (Figure 6C). Considering all of these variables together, elevation is the most important variable at all

sites except for Shorthair, which has a relatively small elevation range (Figure 8). Aspect exerts a stronger influence than do slope and penetration fraction in open areas. However, for under-canopy areas, penetration is more dominant than aspect at two sites. The multivariate regression model was fitted to the data with aspect transformed into 0° to 180° range (north to south). Fitted models could be represented as the following two equations for open area and under canopy respectively,

$$SD = 0.0011 \times Elevation - 0.0112 \times Slope - 0.0057 \times Aspect + 0.1802 \times Penetration \quad (2)$$

$$SD = 0.0009 \times Elevation - 0.0128 \times Slope - 0.0046 \times Aspect + 0.9891 \times Penetration \quad (3)$$

where SD is snow depth and p-values of all regression coefficients of the two models are all smaller than 0.01.

The snow-depth difference between open and canopy-covered area was calculated with elevation from locally smoothed snow depth (Figure 7). It generally increases from near zero at 1500 m, where there is little snow but dense canopy, to 40 cm in the range of 2000-2400 m, and varies from near zero to 60 cm at higher elevations where snow is deeper and the canopy less dense. It is apparent that the snow-depth difference increases with elevation in the rain-snow transition zone, but lacks a clean pattern along either elevation gradient or penetration-fraction gradient when the elevation is higher.

4. Discussion

4.1 Sensitivity of measurements to sampling resolution

The results of the percentage of pixels with snow depth measured from Lidar data at different sampling resolutions illustrate that even high-density airborne Lidar measurements do not have 100% coverage of the surveyed area at 1-m resolution, especially in densely forested areas. According to the snow-depth difference between snowpack in open areas and under

canopy, the trade-off between accuracy and coverage happens when adjusting the resolution; and lower sampling resolutions can introduce overestimation into the results. This is because upon averaging, sub-pixel area under the canopy that was not measured is represented by the open that is measured, introducing an overestimation error into the averaged snow depth of the pixel. Therefore, the sampling resolution for processing the Lidar point cloud needs to be chosen according to the objective and accuracy tolerance of the study.

4.2 Physiographic effect on snow accumulation

Below 3300 m, the increasing trend of snow accumulation with elevation was observed for all sites (Figure 5). Linear regression is applicable to model the relationship between snow depth and elevation when the study area has a broad elevation range. This holds true for all of our sites with the exception of Shorthair, where the elevation range is about 200 m and the coefficient of determination for this linear model is much smaller than the other three sites, which have ranges greater than 500 m. The bias of mean snow depth in the same elevation band between different sites is acceptable if the standard error is added or subtracted from the mean (Figure 5a, 5b). The data-collection time, spatial variation and variations of other topographic features should introduce bias across sites. However, as data-collection time only differs a few days, *in situ* snow-depth sensor data suggest that the melting and densification effect was under 2 cm (https://czo.ucmerced.edu/dataCatalog_sierra.html). Spatial variations at 1800-2000 m elevations between Providence and the further-south Wolverton site appear to have a consistent bias, with less precipitation falling in the southerly location. As for other topographic variables, the observation of a slope effect, shown as the trend lines in Figure 6a and the negative regression coefficients of the two linear models, could be explained by steeper slopes having higher avalanche potential, fewer trees and thus more wind; and thus some snow is more likely

to be lost from these slopes. Snowpack located in south-facing slopes receives higher solar radiation, with the snowmelt being accelerated (Kirchner et al., 2014). This explains the trends observed in Figure 6b and the negative regression coefficients of the multivariate models. Although Lidar has measurement errors caused by slope and aspect (Baltsavias, 1999; Deems et al., 2013; Hodgson and Bresnahan, 2004), error is not able to be quantified and traced back to each variable and we assumed its influence on the trends could be neglected. As canopy interception results in reduced snow depth under canopy, the snow-depth residuals are found increasing with penetration fraction and the regression coefficients are positive (Figure 6c). The multivariate linear regression model built from the Lidar data is a significant improvement, as the variability of the snowpack distribution could explain 15 to 25% more than the univariate linear regression model with elevation as the only predictive variable (Table 4) and the estimation bias has a narrower distribution (Figure 9a, 9b). Also, fitting an individual linear model for each site is slightly better than using a general model with all sites' data involved (Figure 9c, d) and it might because that an individual model could capture regional micro-climate within the site better than a general model. The opposite trend of the relative importance of predictive variables observed in Shorthair is because it is a relatively flat site (Figure 1, Figure 8), which implies that topographic variables other than elevation need to be focused more when studying about areas with small elevation ranges in future works.

4.3 Vegetation effects on snow accumulation along elevation

Under-canopy snow distribution is governed by multiple factors that affect the energy environment, as observed by melting (Essery et al., 2008; Gelfan et al., 2004) and accumulation rates (Pomeroy et al., 1998; Schmidt and Gluns, 1991; Teti, 2003). Our results show different responses when comparing the snow-depth difference between open and canopy-covered areas

between study sites (Figure 7c). In the rain-snow transition zone from 1500 to 2000 m of Providence we see a sharp linear increase between open and under-canopy accumulation that is likely governed by the under-canopy energy environment and the canopy-interception effect on precipitation, which accelerate snowmelt and prevent accumulation of under-canopy snow. Above 2000 m, the snow-depth difference observed at Bull and Shorthair stabilized around 40 cm and 20 cm respectively, with fluctuations less than 10 cm along elevation. Breaking from this pattern, the large dip in snow-depth difference, down to 10 cm, observed at Wolverton at elevations of 2250 - 2750 m deviates from the 35-40 cm plateau. Also, the snow-depth difference at Shorthair stabilizes around 20 cm, which is 20 cm lower than the stabilized value at Bull. Based on the scatterplot in Figure 7a and 7b that color coded by northness, at elevation range of 2300 m to 2700 m, there are a lot more data points with both low snow depth and extremely negative northness in the open area than under the canopy, which implies that anisotropic distribution of other topographic variables is affecting the snow-depth difference. This is further shown by filtering out the data points not within a small certain range (-0.1 to 0.1) of northness, and then reproducing Figure 7c using the filtered data. As presented in Figure 10, it is apparent that the large dip at Wolverton is flattened out to a canopy effect of around 25-45 cm as the topographic effect is filtered out. Thus a sigmoidal function was used to characterize the snow-depth difference changes with elevation excluding topographic interactions. The interactions between topographic variables and vegetation is most likely attributable to the under-canopy snowpack being less sensitive to solar radiation versus snowpack in the open area (Courbaud et al., 2003; Dubayah, 1994; Essery et al., 2008; Musselman et al., 2008, 2012).

In spite of filtering the topographic effect, there is still about a 20-cm magnitude of fluctuation in the snow-depth difference, which might be attributed to various clearing sizes of

open area at different locations and various vegetation types in the forests (Hedstrom and Pomeroy, 1998; Pomeroy et al., 2002; Schmidt and Gluns, 1991), however, these features of the sites are not able to be explored from this Lidar data set.

5. Conclusions

As an advanced and promising remote-sensing technology, Lidar is able to measure snow depth of 100% survey area at 5-m sampling resolution however the accuracy is still left to be evaluated because of lacking enough representative measurements under the canopy. A 1-m resolution processed Lidar data set is more accurate but the percentage of pixels with measurements is much less than 100%.

Using processed Lidar data sampled at 1-m resolution, averaged snow depth within each 1-m elevation band shows a strong correlation with elevation at all sites, indicating that snow accumulation in the southern Sierra Nevada is primarily affected by orographic lift. Snow-depth residuals calculated by de-trending the elevation dependency are correlated with slope, aspect and penetration fraction, which shows the effect of additional physiographic variables on snow accumulation other than elevation. The relative importance of these variables in predicting snow depth implies that other than elevation, aspect affects snow-accumulation and retention more in open areas, while penetration fraction is as important as aspect for snow under the canopy. More significantly, a multivariate linear regression model fitted with variables for slope, aspect and canopy penetration fraction explains 15 to 25% more snow-depth variability than using elevation as the only predictive variable, suggesting multiple predictive variables will be more effective for quantifying the water equivalent in the Sierra Nevada at peak snow accumulation.

The snow-depth difference between open and canopy-covered areas increases in the rain-snow transition elevation range and then stabilized around 25 to 45 cm at high elevation. Large

373 magnitude of fluctuations are presented at certain elevation ranges in Wolverton and Shorthair,
374 which is partially due to interactions from other topographic variables, evidence of which is
375 found by filtering the northness into a narrow band and which causes the fluctuations flattening
376 out.

Acknowledgements. This material is based on data and processing services provided by the OpenTopograhy Facility with support from the National Science Foundation under NSF Award Numbers 1226353 & 1225810. Research was supported by the National Science Foundation under NSF Award Numbers 1331939 & 1239521. We acknowledge the helpful comments from Q. Guo, A. Harpold, and N.P. Molotch, also Q. Guo and J. Flanagan for providing canopy height model data.

Reference

Anderson, H. W.: Managing California's Snow Zone Lands for Water, Pacific Southwest For. Range Exp. Station. Berkeley, CA, 34, 1963.

Bales, R. C., Molotch, N. P., Painter, T. H., Dettinger, M. D., Rice, R. and Dozier, J.: Mountain hydrology of the western United States, Water Resour. Res., 42(8), n/a–n/a, doi:10.1029/2005WR004387, 2006.

Bales, R. C., Hopmans, J. W., O'Geen, A. T., Meadows, M., Hartsough, P. C., Kirchner, P., Hunsaker, C. T. and Beaudette, D.: Soil Moisture Response to Snowmelt and Rainfall in a Sierra Nevada Mixed-Conifer Forest, Vadose Zo. J., 10(3), 786, doi:10.2136/vzj2011.0001, 2011.

Baltsavias, E.: Airborne laser scanning: basic relations and formulas, ISPRS J. Photogramm. Remote Sens., (54), 199–214 [online] Available from: http://www2.geog.ucl.ac.uk/~mdisney/teaching/teachingNEW/PPRS/papers/Baltsavias_Lidar.pdf, 1999.

Barrett, A. P.: National Operational Hydrologic Remote Sensing Center SNOw Data Assimilation System (SNODAS) Products at NSIDC, NSIDC Spec. Rep. 11, (Natl. Snow and Ice Data Cent.: Boulder, CO), 19, 2003.

Breiman, L. (University of C.: Random forest, Mach. Learn., 45(1), 5–32, doi:10.1023/A:1010933404324, 2001.

Cleveland, W. S.: Robust Locally Weighted Regression and Smoothing Scatterplots, J. Am. Stat. Assoc., 74(368), 829–836, doi:10.2307/2286407, 1979.

Clow, D. W., Nanus, L., Verdin, K. L. and Schmidt, J.: Evaluation of SNODAS snow depth and snow water equivalent estimates for the Colorado Rocky Mountains, USA, Hydrol. Process., 26(17), 2583–2591, doi:10.1002/hyp.9385, 2012.

Colle, B. a.: Sensitivity of Orographic Precipitation to Changing Ambient Conditions and Terrain Geometries: An Idealized Modeling Perspective, J. Atmos. Sci., 61(5), 588–606, doi:10.1175/1520-0469(2004)061<0588:SOOPTC>2.0.CO;2, 2004.

Courbaud, B., De Coligny, F. and Cordonnier, T.: Simulating radiation distribution in a heterogeneous Norway spruce forest on a slope, Agric. For. Meteorol., 116(1-2), 1–18, doi:10.1016/S0168-1923(02)00254-X, 2003.

Deems, J. S. and Painter, T. H.: Lidar measurement of snow depth: accuracy and error sources, Proc. 2006 Int. Snow Sci. Work. Telluride, Color. USA, Int. Snow Sci. Work., 330, 330–338, 2006.

Deems, J. S., Fassnacht, S. R. and Elder, K. J.: Fractal Distribution of Snow Depth from Lidar Data, J. Hydrometeorol., 7(2), 285–297, 2006.

Deems, J. S., Painter, T. H. and Finnegan, D. C.: Lidar measurement of snow depth: a review, J. Glaciol., 59(215), 467–479, doi:10.3189/2013JoG12J154, 2013.

Dubayah, R. C.: Modeling a solar radiation topoclimatology for the Rio Grande River Basin, J. Veg. Sci., 5(5), 627–640, doi:10.2307/3235879, 1994.

Erickson, T. a., Williams, M. W. and Winstral, A.: Persistence of topographic controls on the spatial distribution of snow in rugged mountain terrain, Colorado, United States, Water Resour. Res., 41(4), 1–17, doi:10.1029/2003WR002973, 2005.

Erxleben, J., Elder, K. and Davis, R.: Comparison of spatial interpolation methods for estimating snow distribution in the Colorado Rocky Mountains, Hydrol. Process., 16(18), 3627–3649, doi:10.1002/hyp.1239, 2002.

Essery, R., Bunting, P., Rowlands, A., Rutter, N., Hardy, J., Melloh, R., Link, T., Marks, D. and Pomeroy, J.: Radiative Transfer Modeling of a Coniferous Canopy Characterized by Airborne Remote Sensing, J. Hydrometeorol., 9(2), 228–241, doi:10.1175/2007JHM870.1, 2008.

Gelfan, a. N., Pomeroy, J. W. and Kuchment, L. S.: Modeling Forest Cover Influences on Snow Accumulation, Sublimation, and Melt, J. Hydrometeorol., 5(5), 785–803, doi:10.1175/1525-7541(2004)005<0785:MFCIOS>2.0.CO;2, 2004.

Goulden, M. L., Anderson, R. G., Bales, R. C., Kelly, a. E., Meadows, M. and Winston, G. C.: Evapotranspiration along an elevation gradient in California's Sierra Nevada, J. Geophys. Res. Biogeosciences, 117(3), 1–13, doi:10.1029/2012JG002027, 2012.

Grünewald, T., Stötter, J., Pomeroy, J. W., Dadic, R., Moreno Baños, I., Marturià, J., Spross, M., Hopkinson, C., Burlando, P. and Lehning, M.: Statistical modelling of the snow depth distribution in open alpine terrain, Hydrol. Earth Syst. Sci., 17(8), 3005–3021, doi:10.5194/hess-17-3005-2013, 2013.

Grünewald, T., Bühler, Y. and Lehning, M.: Elevation dependency of mountain snow depth, Cryosph., 8(6), 2381–2394, doi:10.5194/tc-8-2381-2014, 2014.

Guan, B., Molotch, N. P., Waliser, D. E., Jepsen, S. M., Painter, T. H. and Dozier, J.: Snow water equivalent in the Sierra Nevada: Blending snow sensor observations with snowmelt model simulations, Water Resour. Res., 49(August), 5029–5046, doi:10.1002/wrcr.20387, 2013.

Hedstrom, N. R. and Pomeroy, J. W.: Measurements and modelling of snow interception in the boreal forest, Hydrol. Process., 12(10-11), 1611–1625, doi:10.1002/(SICI)1099-

1085(199808/09)12:10/11<1611::AID-HYP684>3.0.CO;2-4, 1998.

Hodgson, M. E. and Bresnahan, P.: Accuracy of Airborne Lidar-Derived Elevation : Empirical Assessment and Error Budget, Photogramm. Eng. Remote Sensing, 70(3), 331–339, 2004.

Hopkinson, C., Sitar, M., Chasmer, L., Gynan, C., Agro, D., Enter, R., Foster, J., Heels, N., Hoffman, C., Nillson, J. and Others: Mapping the spatial distribution of snowpack depth beneath a variable forest canopy using airborne laser altimetry, Proc. 58th Annu. East. Snow Conf., 2001.

Hopkinson, C., Sitar, M., Chasmer, L. and Treitz, P.: Mapping snowpack depth beneath forest canopies using airborne lidar., Photogramm. Eng. Remote Sens., 70(3), 323–330, 2004.

Howat, I. M. and Tulaczyk, S.: Trends in spring snowpack over a half-century of climate warming in California, USA, Ann. Glaciol., 40, 151–156, doi:10.3189/172756405781813816, 2005.

Hunsaker, C. T., Whitaker, T. W. and Bales, R. C.: Snowmelt Runoff and Water Yield Along Elevation and Temperature Gradients in California's Southern Sierra Nevada1, JAWRA J. Am. Water Resour. Assoc., 48(4), 667–678, doi:10.1111/j.1752-1688.2012.00641.x, 2012.

J. Revuelto, J. I. Lo?pez-Moreno, C. A.-M. and Vicente-Serrano, S. M.: Canopy influence on snow depth distribution in a pine stand determined from terrestrial laser data, Water Resour. Res., doi:10.1002/2014WR016496, 2015.

Kirchner, P. B., Bales, R. C., Molotch, N. P., Flanagan, J. and Guo, Q.: LiDAR measurement of seasonal snow accumulation along an elevation gradient in the southern Sierra Nevada, California, Hydrol. Earth Syst. Sci. Discuss., 11, 5327–5365, doi:10.5194/hessd-11-5327-2014, 2014.

Lehning, M., Grünewald, T. and Schirmer, M.: Mountain snow distribution governed by an altitudinal gradient and terrain roughness, Geophys. Res. Lett., 38(19), 1–5, doi:10.1029/2011GL048927, 2011.

Mahat, V. and Tarboton, D. G.: Representation of canopy snow interception, unloading and melt in a parsimonious snowmelt model, Hydrol. Process., 6336(December 2013), n/a–n/a, doi:10.1002/hyp.10116, 2013.

Marks, K. and Bates, P.: Integration of high-resolution topographic data with floodplain flow models, Hydrol. Process., 14(July 1998), 2109–2122, doi:10.1002/1099-1085(20000815/30)14:11/12<2109::AID-HYP58>3.0.CO;2-1, 2000.

McMillen, R. T.: An eddy correlation technique with extended applicability to non-simple terrain, Boundary-Layer Meteorol., 43(3), 231–245, doi:10.1007/BF00128405, 1988.

Molotch, N. P. and Margulis, S. a.: Estimating the distribution of snow water equivalent using remotely sensed snow cover data and a spatially distributed snowmelt model: A multi-resolution, multi-sensor comparison, Adv. Water Resour., 31(11), 1503–1514, doi:10.1016/j.advwatres.2008.07.017, 2008.

Molotch, N. P., Colee, M. T., Bales, R. C. and Dozier, J.: Estimating the spatial distribution of snow water equivalent in an alpine basin using binary regression tree models: The impact of digital elevation data and independent variable selection, Hydrol. Process., 19(December 2004), 1459–1479, doi:10.1002/hyp.5586, 2005.

Musselman, K. N., Molotch, N. P. and Brooks, P. D.: Effects of vegetation on snow accumulation and ablation in a mid-latitude sub-alpine forest, Hydrol. Process., 22(15), 2767–2776, doi:10.1002/hyp, 2008.

Musselman, K. N., Molotch, N. P., Margulis, S. a., Kirchner, P. B. and Bales, R. C.: Influence of canopy structure and direct beam solar irradiance on snowmelt rates in a mixed conifer forest, Agric. For. Meteorol., 161, 46–56, doi:10.1016/j.agrformet.2012.03.011, 2012.

Musselman, K. N., Margulis, S. a. and Molotch, N. P.: Estimation of solar direct beam transmittance of conifer canopies from airborne LiDAR, Remote Sens. Environ., 136, 402–415, doi:10.1016/j.rse.2013.05.021, 2013.

Nolan, M., Larsen, C. and Sturm, M.: Mapping snow-depth from manned-aircraft on landscape scales at centimeter resolution using Structure-from-Motion photogrammetry, Cryosph. Discuss., 9, 333–381, doi:10.5194/tcd-9-333-2015, 2015.

Pedregosa, F. and Varoquaux, G.: Scikit-learn: Machine Learning in Python, J. Mach. …, 12, 2825–2830 [online] Available from: http://jmlr.csail.mit.edu/papers/volume12/pedregosa11a/pedregosa11a.pdf, 2011.

Pomeroy, J. W., Parviainen, J., Hedstrom, N. and Gray, D. M.: Coupled modelling of forest snow interception and sublimation, Hydrol. Process., 12(15), 2317–2337, doi:10.1002/(SICI)1099-1085(199812)12:15<2317::AID-HYP799>3.0.CO;2-X, 1998.

Pomeroy, J. W., Gray, D. M., Hedstrom, N. R. and Janowicz, J. R.: Prediction of seasonal snow accumulation in cold climate forests, Hydrol. Process., 16(18), 3543–3558, doi:10.1002/hyp.1228, 2002.

Raupach, M. R.: Vegetation-atmosphere interaction in homogeneous and heterogeneous terrain: some implications of mixed-layer dynamics, Vegetatio, 91(1-2), 105–120, doi:10.1007/BF00036051, 1991.

Rice, R. and Bales, R. C.: Embedded-sensor network design for snow cover measurements around snow pillow and snow course sites in the Sierra Nevada of California, Water Resour.

Res., 46(3), 1–13, doi:10.1029/2008WR007318, 2010.

Rice, R., Bales, R. C., Painter, T. H. and Dozier, J.: Snow water equivalent along elevation gradients in the Merced and Tuolumne River basins of the Sierra Nevada, Water Resour. Res., 47(8), n/a–n/a, doi:10.1029/2010WR009278, 2011.

Roe, G. H.: Orographic Precipitation, Annu. Rev. Earth Planet. Sci., 33(1), 645–671, doi:10.1146/annurev.earth.33.092203.122541, 2005.

Roe, G. H. and Baker, M. B.: Microphysical and Geometrical Controls on the Pattern of Orographic Precipitation, J. Atmos. Sci., 63(3), 861–880, doi:10.1175/JAS3619.1, 2006.

Rosenberg, E. a., Wood, A. W. and Steinemann, A. C.: Statistical applications of physically based hydrologic models to seasonal streamflow forecasts, Water Resour. Res., 47(3), n/a–n/a, doi:10.1029/2010WR010101, 2011.

Rotach, M. W. and Zardi, D.: On the boundary-layer structure over highly complex terrain: Key findings from MAP, Q. J. R. …, 133, 937–948, doi:10.1002/qj, 2007.

Schmidt, R. a. and Gluns, D. R.: Snowfall interception on branches of three conifer species, Can. J. For. Res., doi:10.1139/x91-176, 1991.

Smith, R. B. and Barstad, I.: A Linear Theory of Orographic Precipitation, J. Atmos. Sci., 61(12), 1377–1391, doi:10.1175/1520-0469(2004)061<1377:ALTOOP>2.0.CO;2, 2004.

Teti, P.: Relations between peak snow accumulation and canopy density, For. Chron., 79(2), 307–312, 2003.

Wigmosta, M. S., Vail, L. W. and Lettenmaier, D. P.: A distributed hydrology-vegetation model for complex terrain, Water Resour. Res., 30(6), 1665–1680, doi:10.1029/94WR00436, 1994.

1 Table 1. LiDAR data collection information

	Snow-off flight date	Snow-on flight date	Area, km^2
Bull	August 15, 2010	March 24, 2010	22.3
Shorthair	August 13, 2010	March 23, 2010	6.8
Providence	August 5, 2010	March 23, 2010	18.4
Wolverton	August 13-15, 2010	March 21-22, 2010	58.9

2 Table 2. Flight parameters and sensor settings

Flight parameters		Equipment settings	
flight altitude	600 m	wavelength	1047 nm
flight speed	65 m s^{-1}	beam divergence	0.25 mrad
swath width	233.26 m	laser PRF	100 kHz
Swath overlap	50%	scan frequency	55 Hz
point density	10.27 p m^{-2}	scan angle	±14°
Cross track res	0.233 m	scan cutoff	3°
Down track res	0.418 m	scan offset	0°

3 Table 3. Linear regression of averaged snow depth vs. elevation in four sites

	Bull	Shorthair	Providence	Wolverton
Open R^2	0.968	0.797	0.931	0.914
Vegetated R^2	0.978	0.737	0.921	0.972
Open slope, cm per 100 m	21.6	16.1	37.8	15.3
Vegetated slope, cm per 100 m	19.9	13.1	26.0	13.4

4 Table 4. Coefficients of determination of univariate and multivariate linear models

	Univariate model R^2	Multivariate model R^2
Bull	0.23	0.37
Shorthair	0.06	0.32
Providence	0.39	0.53
Wolverton	0.16	0.38
All sites	0.43	0.57

5

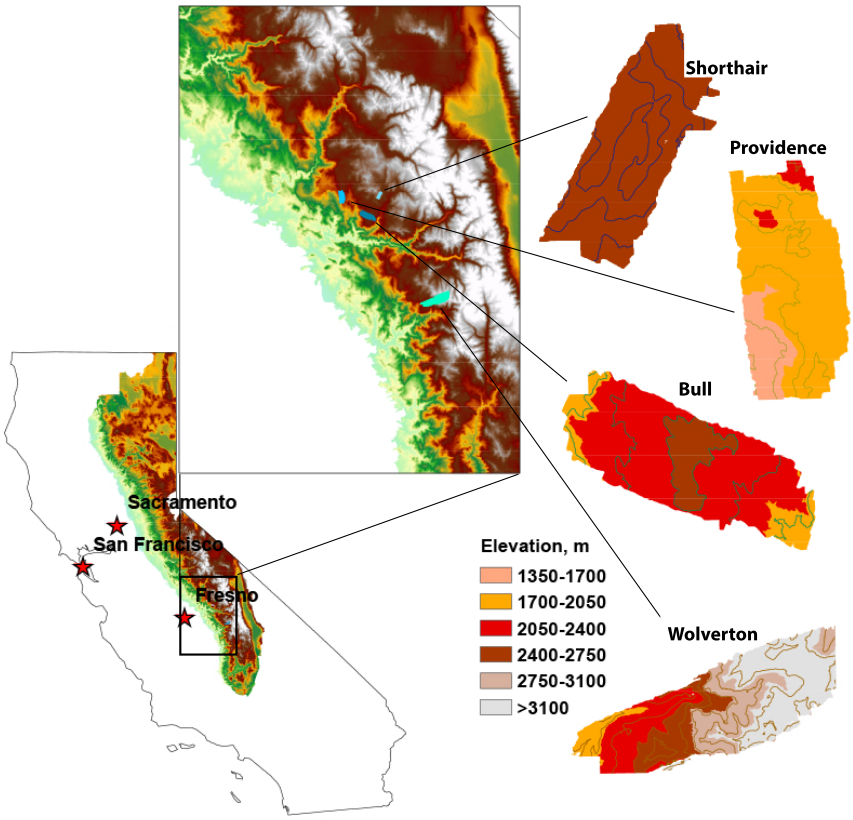

Figure 1. Study area and Lidar footprints. (Left) California with Sierra Nevada. (Center) Zoomed view to show the locations of Lidar footprints. (Right) Elevation and 200-m contour map (100-m for Bull) of LiDAR footprints

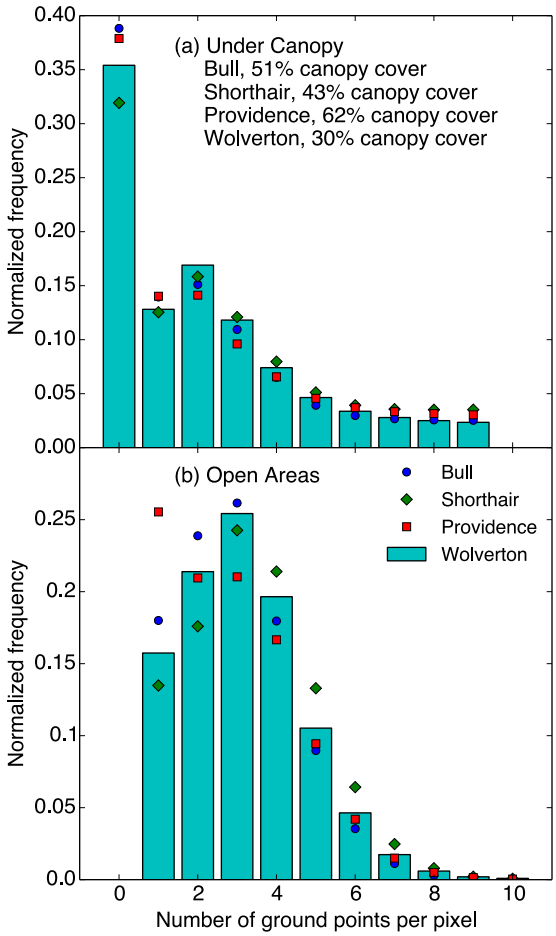

10

11 Figure 2. (a) Normalized histogram of the number of ground points for under canopy pixels. (b)
12 Normalized histogram of the number of ground points in open pixels.

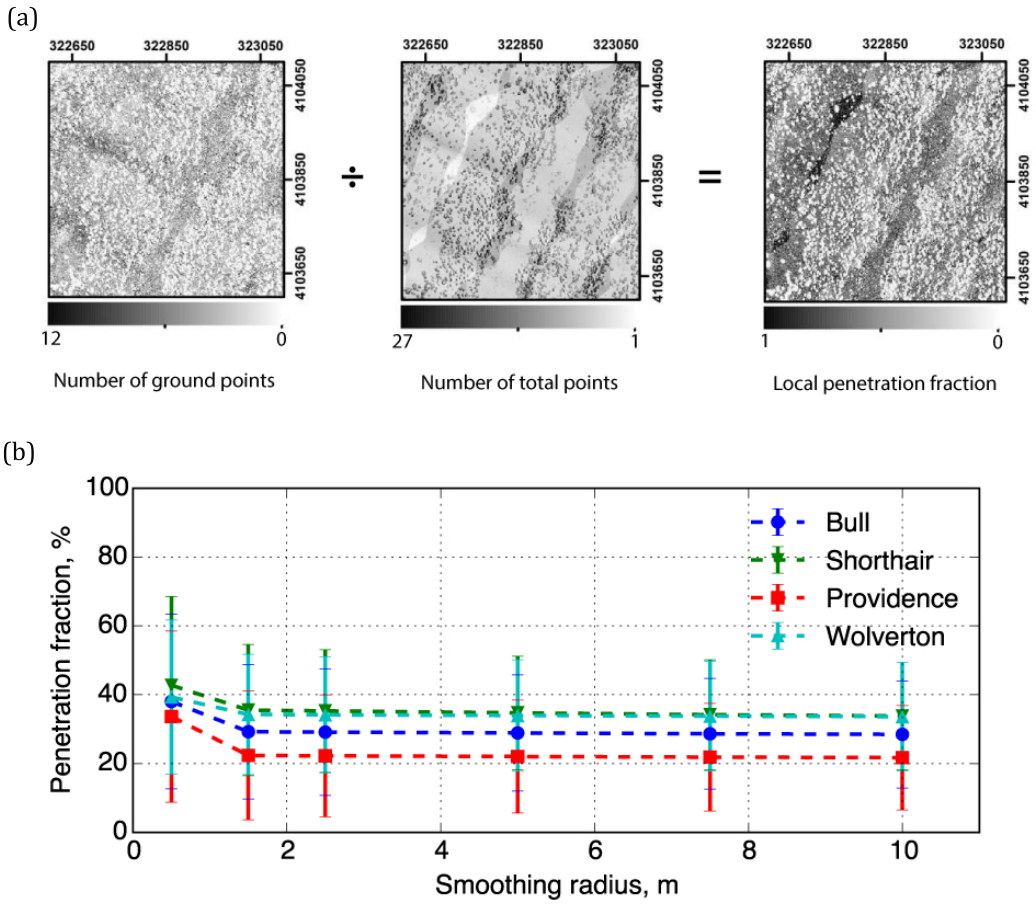

Figure 3. (a) Dividing the number of ground points of each 1-m pixel by the total number of points in the pixel will result the penetration fraction of the local pixel. (b) Sensitivity of the smoothed penetration fraction to the smoothing radius, showing that the result is not sensitivity as the radius is larger than 1.5 m.

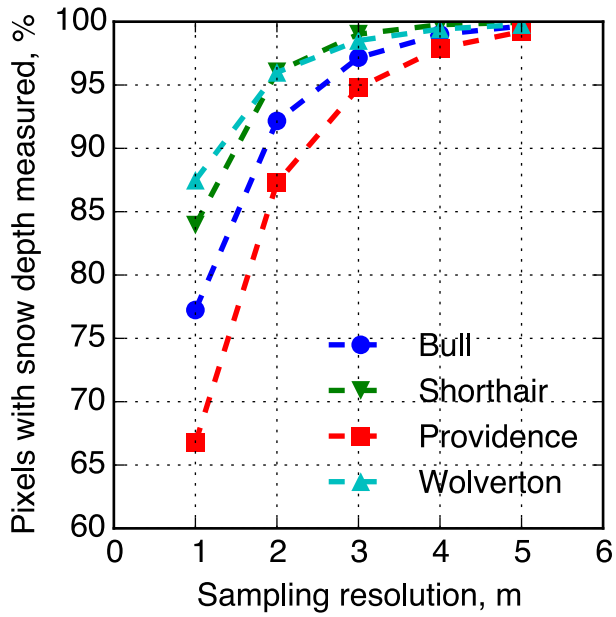

Figure 4. Sensitivity of the percentage of pixels with snow depth measured to the sampling resolution used in processing the Lidar point cloud at each site.

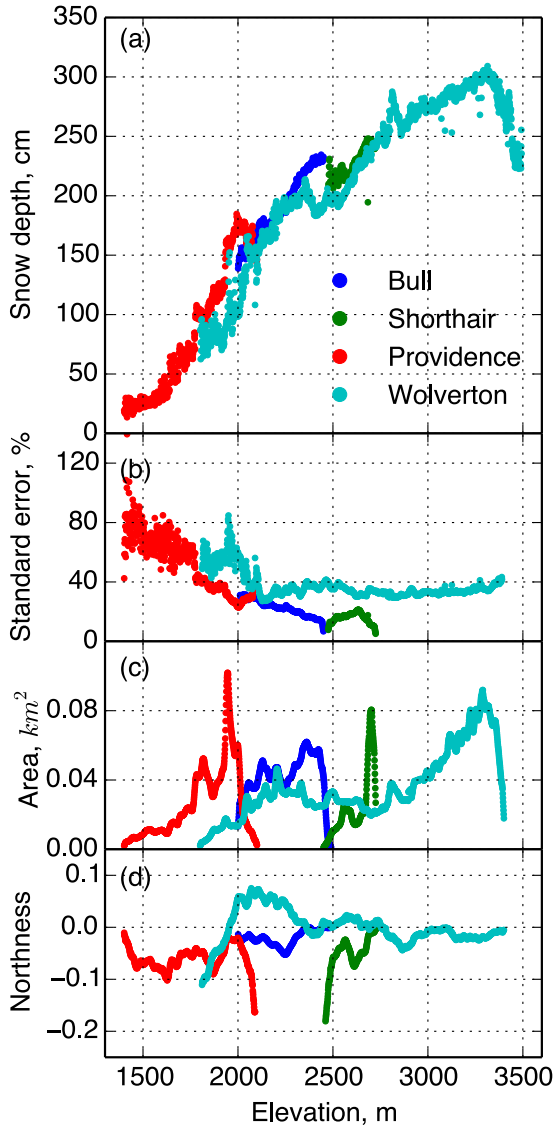

Figure 5. (a) Averaged snow depth from snow-on and snow-off Lidar data versus elevation for pixels in the open at the four sites. (b) Standard error of the snow depth within each 1-m elevation band. Values above 3400 m not shown, where there are few data. (c) Total area of averaged data within each elevation band. (d) Averaged northness of each elevation band from four sites.

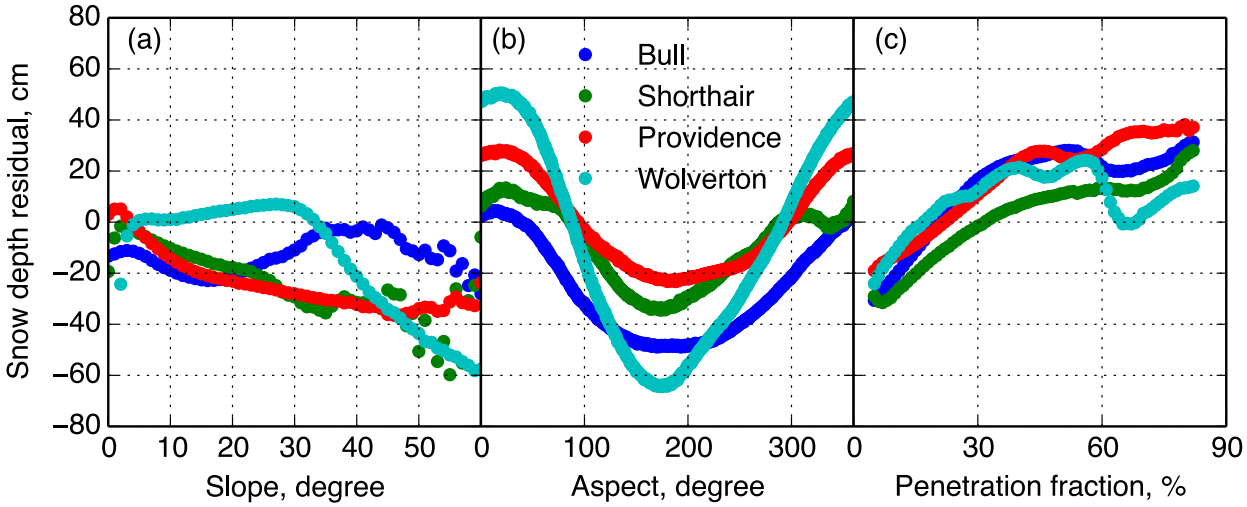

Figure 6. (a) Averaged snow-depth residual along slope. Raw snow-depth residual was calculated from Lidar measured snow depth and estimated snow depth from the linear regression model (open areas). (b) Averaged snow-depth residual along aspect. (c) Averaged snow-depth residual along penetration fraction.

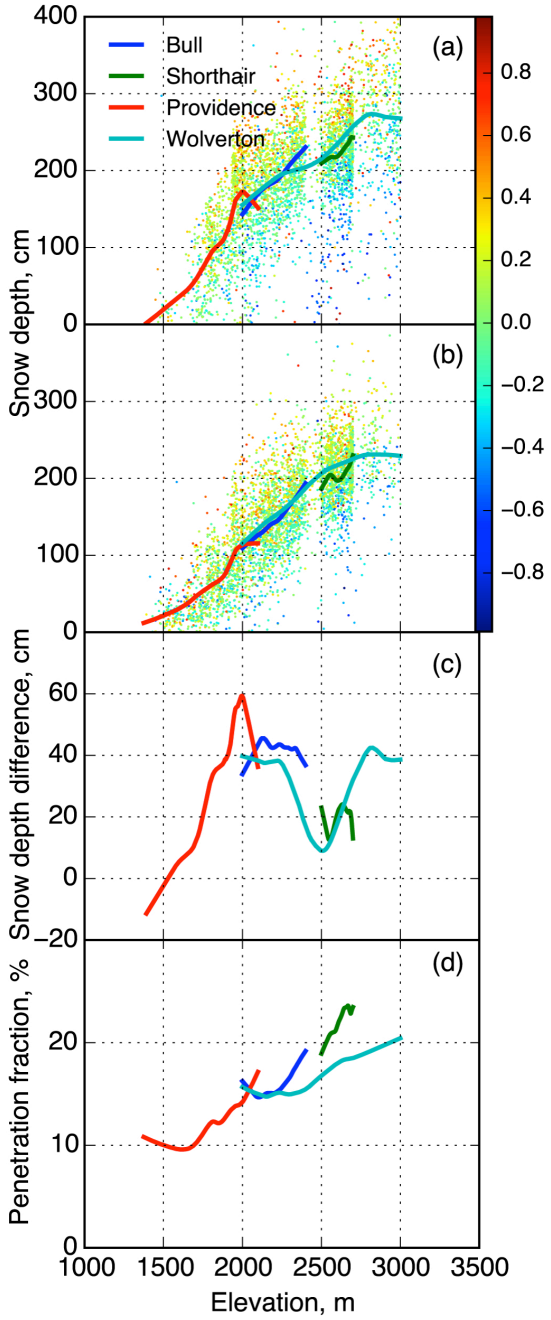

Figure 7. LOESS smoothed snow depth with northness color coded scatterplot of raw-pixel snow depth against elevation for (a) open area (b) canopy-covered area. (c) Snow-depth difference along elevation calculated from the LOESS smoothed snow depth. (d) Averaged penetration fraction.

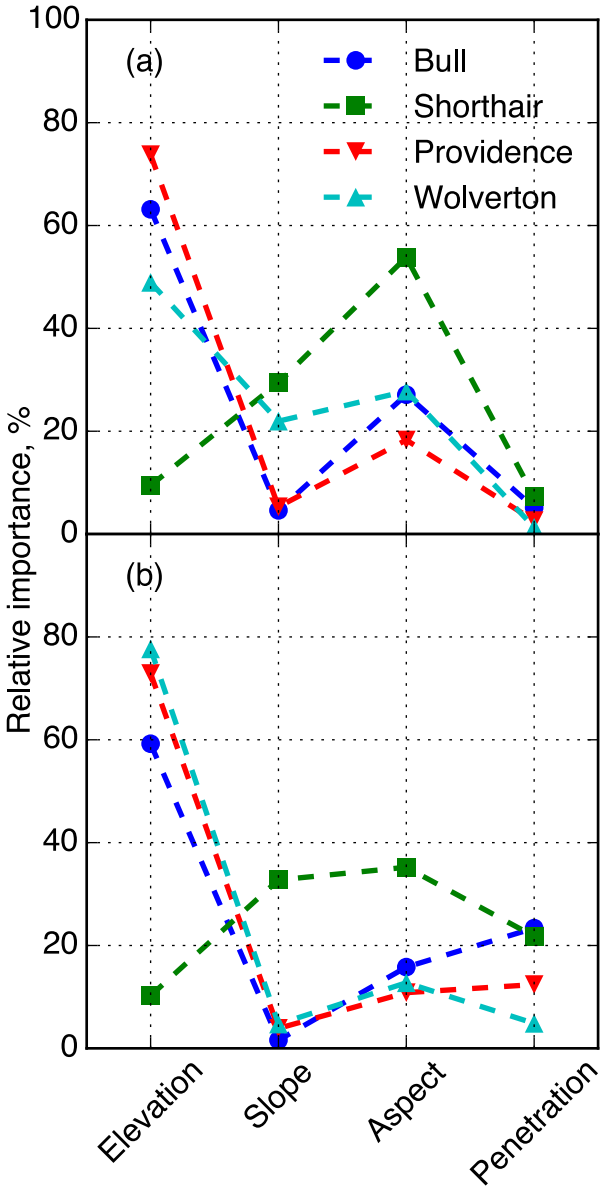

Figure 8. Relative importance of each physiographic variable in predicting the snow depth from each site for (a) open area (b) canopy-covered area

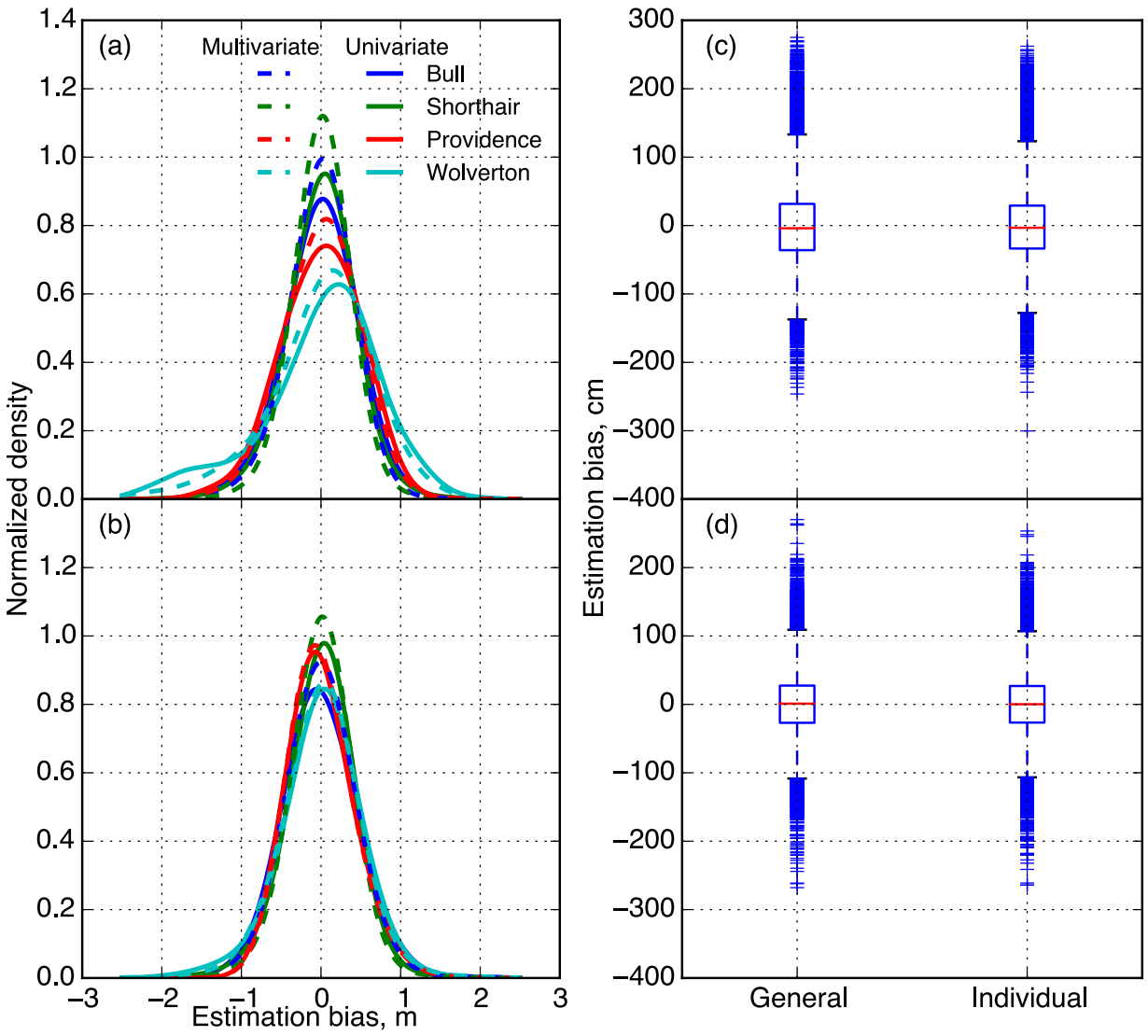

36

37 Figure 9. Normalized density of estimation bias for (a) open area (b) canopy-covered area; Estimation
38 bias boxplots of using one general linear model with all sites' data combined and four linear models of
39 each individual site for (c) open area (d) canopy-covered area.

40

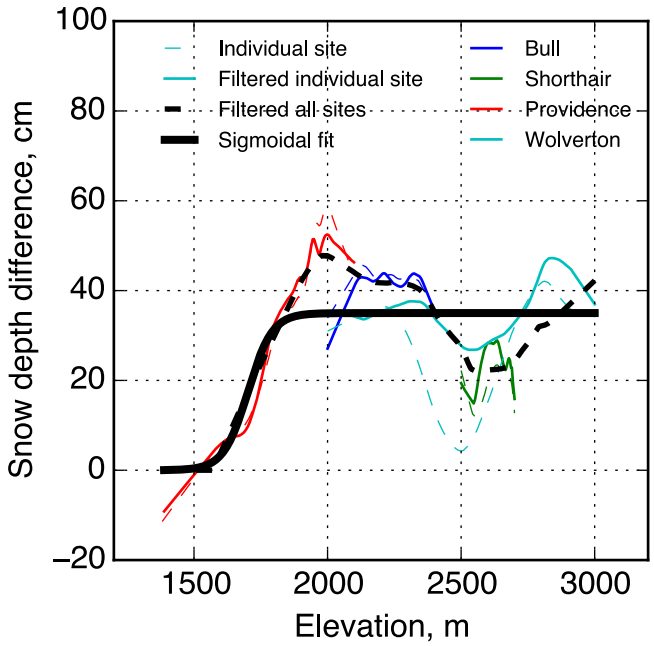

41

42 Figure 10. Snow-depth difference between open and canopy-covered area: comparison between
43 using raw 1-m pixel snow depth and northness-filtered 1-m pixel snow depth, together with the
44 sigmoidal fit of the snow-depth difference changing with elevation

45